

# <sup>131</sup>I-Rituximab: Relationship Between Immunoreactivity and Specific Activity

Andreas O. Schaffland, PhD<sup>1</sup>; Franz Buchegger, MD<sup>1,2</sup>; Marek Kosinski, PhD<sup>1</sup>; Cristian Antonescu, MD<sup>1</sup>; Corinne Paschoud<sup>1</sup>; Carine Grannavel, MSc<sup>1</sup>; Raimo Pellikka<sup>3</sup>; and Angelika Bischof Delaloye, MD<sup>1</sup>

<sup>1</sup>Division of Nuclear Medicine, University Hospital of Lausanne, Lausanne, Switzerland; <sup>2</sup>Division of Nuclear Medicine, University Hospital of Geneva, Geneva, Switzerland; and <sup>3</sup>Center for Radiopharmaceutical Science, Paul-Scherrer-Institute, Villigen, Switzerland

As part of a search for optimal conditions for radioimmunotherapy of lymphoma, rituximab was labeled with 2 different specific activities of <sup>131</sup>I and immunoreactivity was comparatively measured. **Methods:** Labeling was performed with chloramine T using as starting conditions 185 MBq of <sup>131</sup>I per 1 mg and per 5 mg of antibody for labelings A and B, respectively. Six comparative labelings were performed over a period of 10 mo with similar efficacy and purified by anion-exchange chromatography. Immunoreactivity was determined immediately after labeling in parallel assays using different concentrations of fresh Raji and Daudi cells. Results were compared at maximal observed specific binding on 10<sup>7</sup> cells and after extrapolation to infinite antigen excess. A statistical analysis was performed to predict the frequency of radiolabeled mono- and polyiodinated antibodies: First, a gaussian distribution predicted the number of iodine atoms per antibody in labelings A and B, respectively; then, the radiolabeling probability was developed according to the Newton binome. **Results:** Final radiochemical purity was >98.4% for all labelings. The final mean specific activities were 169.7 MBq/mg and 32.8 MBq/mg, corresponding to 0.87 and 0.17 iodine atoms per antibody in labelings A and B, respectively. Labeling B showed a significantly higher immunoreactivity than did labeling A, the mean relative increase in binding being ≥28% for both Raji cells and Daudi cells. The predictive statistical analysis indicated that 57.3% and 15.4% of radiolabeled antibodies in labelings A and B, respectively, were polyiodinated. **Conclusion:** The low specific activity of <sup>131</sup>I-rituximab allowed preservation of a high immunoreactivity and correlated with the prediction of a low percentage of polyiodinated radio-labeled antibodies.

**Key Words:** rituximab; radioiodination; immunoreactivity; polyiodination

**J Nucl Med 2004; 45:1784–1790**

**R**ituximab (MabThera; F. Hoffmann-La Roche Ltd./Rituxan; IDEC Pharmaceuticals Inc.), a chimeric IgG1 κ-monoclonal antibody (mAb) directed against the cluster

designation 20 (CD20) antigen (1–3), was approved in 1998 by the U.S. Food and Drug Administration for immunotherapy of non-Hodgkin's B-cell lymphoma. Low immunogenicity of the antibody has been observed, with human antimurine or antichimeric antibodies developing in less than 1% of patients after multiple injections (2).

Different groups have already reported on the use of <sup>131</sup>I-labeled rituximab in radioimmunotherapy (4,5). With the intention to develop a repeated radioimmunotherapy, we performed a <sup>131</sup>I-labeling study of rituximab using 2 different radioiodination degrees. On the basis of literature reports (4–6), we chose the labeling starting conditions of 185 MBq/1 mg of antibody and 185 MBq/5 mg of antibody for labelings A and B, respectively. Labeling was performed using an optimized chloramine T (*N*-chloro-4-toluenesulfonamide) method (7) followed by purification with anion-exchange resin. Because labeling A was designed for use in a pharmacokinetic study of patients (8), and because immunoreactivity of an antibody is a most important parameter when used in therapy (9), fine-tuning of the labeling conditions had been performed to preserve the immunoreactivity. However, impairment of immunoreactivity can also arise from the antibody iodination degree or impurities of the radioiodine, and different IgGs can be variably affected (6). The paired labelings A and B, performed over a longer time and analyzed in a paired assay for immunoreactivity, should therefore allow determination of the optimal radioiodination condition for rituximab.

Labelings A and B were analyzed statistically to predict the number of mono- and polyiodinated antibodies and the radiolabeling frequency of these fractions. Compared with monoiodinated antibodies, radiolabeled polyiodinated antibodies might contribute to a decreased immunoreactivity.

## MATERIALS AND METHODS

No-carrier-added Na<sup>131</sup>I (≥222 GBq/mg of iodine at calibration time, ≥99.9% radionuclide purity) in phosphate buffer, pH 7, was from MDS Nordion S.A. Rituximab was kindly provided by Roche Pharma. Chemicals and solvents were p.a. grade and purchased from Merck and Fluka. 0.9% NaCl solution was from B. Braun Medical AG, and sterile 0.15 mol/L phosphate buffer, pH 7.0, was from the pharmacy of our hospital. Phosphate-buffered saline, pH 7, for high-pressure liquid chromatography (HPLC) was 58.8

Received Sep. 25, 2003; revision accepted Apr. 23, 2004.  
For correspondence or reprints contact: Franz Buchegger, MD, Division of Nuclear Medicine, Rue de Bugnon 46, CH-1011 Lausanne, Switzerland.  
E-mail: franz.buchegger@chuv.hospvd.ch

mmol/L Na<sub>2</sub>HPO<sub>4</sub>, 41.2 mmol/L KH<sub>2</sub>PO<sub>4</sub>, 100 mmol/L NaCl, and 0.1% (w/v) NaN<sub>3</sub> in bidistilled water. MILLEX-GV 0.22- $\mu$ m sterile filters were from Millipore Corp. Analytic size-exclusion HPLC was performed on a guard-protected TSK 3000 SW gel column, 300  $\times$  7 mm (Toyo Soda Manufacturing Co.). The HPLC system was a model 5000 from Varian Associates, Inc., with ultraviolet detector. The radioactivity monitor was a model 507 B from Berthold LB. Instant thin-layer liquid chromatography (ITLC) paper was from PALL Corp. Thin-layer chromatograms were scanned on a model 284 linear analyzer from Berthold LB. Dose activity was measured with an Atomlab 100 dose calibrator (Biodex). Raji and Daudi cells were cultured in RPMI 1640 with GlutaMAX-I (Invitrogen Corp.), supplemented with 10% heat-inactivated fetal calf serum and penicillin–streptomycin (0.1 mg/mL; Life Technologies, Inc.) in humidified atmosphere at 37°C and 5% CO<sub>2</sub>. Cells were maintained at exponential growth, with the medium changed 2–3 times per week.

### Radiolabeling A

Two-milliliter columns (Supelco) were filled with 1.8 g of anion exchange resin (1  $\times$  8, 100 mesh; Dowex) and washed with 20 mL of 70% ethanol and 50 mL of sterile 0.9% NaCl solution before use. To 200  $\mu$ L of antibody (2 mg of rituximab) and 370 MBq of Na<sup>131</sup>I solution (diluted to 200  $\mu$ L with phosphate buffer, 0.15 mol/L, pH 7.0), 100  $\mu$ L of freshly prepared chloramine T solution (5 mg of chloramine T in 10 mL of phosphate buffer, 0.15 mol/L, pH 7) were added. After 5 min at room temperature, labeling efficacy was controlled by ITLC (methanol/0.9% saline = 85/15; <sup>131</sup>I-rituximab: start, unbound <sup>131</sup>I-iodide; front). The labeling solution was pumped (peristaltic Pump P-1 with 0.5 mL/min flow; Pharmacia) through the anion-exchange column, and the labeling vial was washed successively with 1 and 2 mL of sterile 0.9% saline that was also passed through the resin filter column into the same vial. The purified, radiolabeled antibody solution was finally filtered through a 0.22- $\mu$ m Millipore sterile filter into a sterile penicillin vial, ready for clinical use.

### Radiolabeling B

The procedures were the same as described for labeling A. One hundred microliters of chloramine T solution were added to 185 MBq of undiluted Na<sup>131</sup>I (20–40  $\mu$ L) and 500  $\mu$ L of the antibody solution (5 mg of rituximab). The final volumes of labelings A and B after filtration were between 2.5 and 3 mL. Quality was controlled by ITLC and HPLC (TSK 3000 SW column; 0.1 mol/L phosphate-buffered saline; 0.6 mL/min flow; 280-nm ultraviolet detection, plus radioactivity detection; retention time of 23.3 min for aggregates, 28.0 min for <sup>131</sup>I-rituximab, and 42.2 min for <sup>131</sup>I).

### Chloramine T Absorption Stress Test

Two milligrams (7.1  $\mu$ mol) of chloramine T trihydrate, dissolved in 1 mL of 0.15 mol/L phosphate buffer and 6.5 mL of 0.9% NaCl solution, were passed through the anion-exchange resin column (as described) at 0.5 mL/min. The column was washed with 3 mL of 0.9% NaCl solution (final volume, 10.5 mL). This solution was tested on HPLC for chloramine T content (Lichro-CART 250-4 column [Merck] with a detection limit of 0.5  $\mu$ g/mL chloramine T trihydrate; 1:1 0.1% acetic acid in water:methanol; 1 mL/min flow; 254-nm ultraviolet detection; retention time of 7.12 min for chloramine T).

### Binding Assay

The immunoreactivity of paired labelings A and B was measured simultaneously in duplicate without delay on the 2 cell lines,

Raji and Daudi, using 5 sequential dilutions of between 10<sup>6</sup> and 10<sup>7</sup> cells in exponential growth (microscopic assessment generally indicated >90% viability). Daudi and Raji cells are known for expression of high amounts of CD20 antigen (10), are easy to cultivate in suspension, and are commercially available (American Type Culture Collection). In our laboratory, the first results of measurement by Scatchard plot of CD20 surface expression indicated the presence of 92,000 binding sites per Daudi cell.

Identical amounts of antibody (6 ng), labeled with 1.0 and 0.2 kBq for labelings A and B, respectively, were incubated at 37°C for 2 h in a volume of 200  $\mu$ L of phosphate-buffered saline (0.15 mol/L NaCl and 0.01 mol/L phosphate buffer, pH 7) containing 5% fetal calf serum and NaN<sub>3</sub> (0.02% w/v). Nonspecific binding, generally less than 3%, was assessed by competition with 100  $\mu$ g of unlabeled antibody and subtracted for determination of specific binding. Specific binding results were analyzed at maximal observed binding on 10<sup>7</sup> cells and using extrapolation to infinite antigen excess according to Lindmo et al. (11). The Student *t* test for paired samples was used for statistical comparison of results.

### Predictive Distribution Statistics of Iodination and Radiolabeling

The mean molar ratio of iodine atoms per antibody was calculated on the basis of a specific activity of 222 GBq/mg for <sup>131</sup>I (according to the manufacturer) and a molecular weight of 145 kDa for rituximab (2). For labeling A, 833 ng of iodine (185 MBq) equals 6.56 nmol, and 1 mg of rituximab equals 6.9 nmol, resulting in an initial I/mAb molar ratio of 0.95. For labeling B, the same calculation led to 0.19 as the initial I/mAb ratio. For mean radiochemical labeling yields of 91.8% and 88.6%, final iodination values gave, therefore, I/mAb molar ratios of 0.87 and 0.17 for labelings A and B, respectively.

The statistical distribution of iodines per antibody was then calculated according to Equation 1 (gaussian distribution probability):

$$P_i(x) = \frac{m}{x!} e^{-m}, \quad \text{Eq. 1}$$

where  $P_i(x)$  = the probability of insertion of  $x$  atoms per antibody molecule,  $m$  = the average number of iodine atoms per antibody molecule, and  $x$  = the number of iodine atoms. No-carrier-added (radionuclide purity  $\geq$  99.9%) <sup>131</sup>I contains only a small percentage of <sup>131</sup>I, with most being <sup>127</sup>I (stable iodine). For the declared specific activity of 222 GBq/mg for <sup>131</sup>I, the fractions of <sup>131</sup>I and <sup>127</sup>I were therefore 0.0455 and 0.9545, respectively.

Because immunoreactivity is measured only for the radiolabeled antibodies in a direct binding assay, the radiolabeling probability of mono- and polyiodinated antibodies was then calculated on the following basis: The distribution probability of <sup>131</sup>I (fraction  $a$ ) and <sup>127</sup>I (fraction  $b$ ) for a given number of iodines ( $x$ ) per antibody can be written as  $(a + b)^x$  (Newton binome). As an example, for a biiodinated antibody the formula resolves in  $a^2 + 2ab + b^2$ , where  $a^2 + 2ab$  represents the probability that the antibody will be radiolabeled by 1 atom <sup>131</sup>I ( $2ab$ ) or 2 atoms <sup>131</sup>I ( $a^2$ ), and  $b^2$  the probability that the antibody will be radiolabeled only with <sup>127</sup>I. The radiolabeling probability  $P_a(x)$  of a given number of iodines per antibody was therefore calculated using Equation 2:

$$P_a(x) = (a + b)^x - b^x. \quad \text{Eq. 2}$$

Combination (by multiplication) of the 2 probabilities,  $P_i(x)$  (representing the occurrence probability of a given number of iodines per mAb) and  $P_a(x)$  (representing the radiolabeling probability of a given number of iodines per mAb), gave the probability  $F(x)$  that a given number of iodines per mAb will occur in radiolabeled form. This final probability, expressed as a percentage of the total fraction of radiolabeled antibodies, allowed us to know the percentage of radiolabeled antibodies statistically expected to exist in monoiodinated and polyiodinated forms.

## RESULTS

### Radiolabeling

Because  $^{131}\text{I}$ -rituximab was later to be prepared for use in patient therapy, a semiautomatic labeling method was chosen to minimize exposure of the staff to radiation. Dowex anion-exchange-column filtration allowed efficient elimination of unbound iodine as well as of chloramine T, whereas no significant loss of antibody was observed. Chloramine T elimination by the anion-exchange column (measured by reversed-phase HPLC) was verified in a stress test using an amount 40-fold higher than that used for radiolabeling (Fig. 1). An alternative method of purification, based on the addition of the same volume of anion-exchange resin into the labeling solution (batch method,  $n = 2$ ) was less efficient in removing free iodine than was column filtration, probably because of a low repartition coefficient. Fine-tuning of the chloramine T concentration optimized the amount of chloramine T trihydrate ( $50 \mu\text{g}$  in  $500 \pm 100 \mu\text{L}$  of labeling solution) containing either 370 MBq of  $^{131}\text{I}$  and 2 mg of antibody (labeling A) or 185 MBq of  $^{131}\text{I}$  and 1 mg of antibody (labeling B) obtained with an incubation time of 5 min at room temperature. For comparison, 6 A and B labelings were studied over a period of 10 mo.  $^{131}\text{I}$  was used within 2 d of calibration. The paired labelings were performed consecutively on the same day, starting with labeling A on 4 occasions, because of clinical priority, and using the reverse order on 2 occasions.

For labeling A, radiochemical yield as determined by ITLC before purification was  $91.8\% \pm 3.6\%$  (Table 1), resulting in a final I/mAb molar ratio of 0.87. The radiochemical purity after ion-exchange chromatography as assessed by ITLC was  $99.1\% \pm 0.5\%$ . These results were confirmed by size-exclusion HPLC, which found a radiochemical purity of  $98.9\% \pm 0.9\%$  for  $^{131}\text{I}$ -rituximab. The percentage of radiolabeled aggregates as determined by HPLC was  $0.6\% \pm 0.5\%$  and not significantly different from the HPLC analytic results for unlabeled antibody. No significant increase in aggregation could be observed after 8 h of storage at  $4^\circ\text{C}$ . After storage for 24 h, some increased aggregate formation was observed, but aggregation remained  $<3\%$ . Other degradation products of the antibody were not observed even after storage for 24 h at  $4^\circ\text{C}$ .

For labeling B, radiochemical yield was  $88.6\% \pm 6.2\%$  (Table 1), resulting in a final I/mAb molar ratio of 0.17. Radiochemical purity after purification was similar to that for labeling A (Table 1).

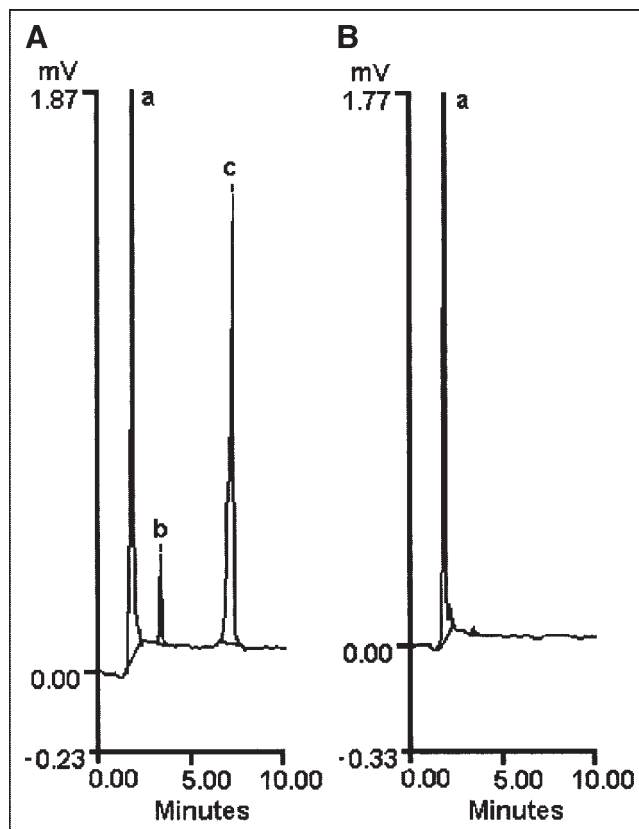


**FIGURE 1.** (A and B) Respective HPLC results before and after anion-exchange-column purification from the chloramine T elimination stress test: void volume (a), unidentified compound (b), and chloramine T (c). A 40-fold higher amount of chloramine T than used in labelings A and B was eliminated from the labeling solution. (The theoretic concentration of chloramine T in the dilution after purification in case of inefficient retention would be  $190 \mu\text{g/mL}$ ; the detection limit was  $0.5 \mu\text{g/mL}$ .)

### Determination of Immunoreactivity

Immunoreactivity was measured comparatively for A and B immediately after labeling using direct binding on fresh Raji and Daudi cells (from the same batches) and background correction for determination of specific binding. Specific binding results were analyzed in 2 ways, once as binding obtained on  $10^7$  Raji and Daudi cells and once using extrapolation to infinite antigen excess according to the method of Lindmo et al. (10) (Table 2). Figure 2 shows a representative experiment for labeling A and B on Raji cells. The results showed a statistically significant higher binding ( $P < 0.03$ ) for labeling B than for labeling A in all 4 comparisons. When combining the results obtained on Raji ( $n = 6$ ) and Daudi cells ( $n = 6$ ) for the paired comparison ( $n = 12$ ), the difference was highly significant ( $P < 0.001$ , Table 2). Detailed reading of the results for the maximal observed binding on  $10^7$  cells and after extrapolation to infinite antigen excess (Table 2) showed that each comparison of the paired labelings gave a higher binding of B than of A, excepting the results for which the extrapolation according to Lindmo indicated an optimal binding of 100% for both.

**TABLE 1**  
Radiochemical Yield Before and Radiochemical Purity After Purification of <sup>131</sup>I-Rituximab

Paired labeling no.	Labeling A		Labeling B	
	% <sup>131</sup> I-Rituximab before purification	% <sup>131</sup> I-Rituximab after purification	% <sup>131</sup> I-Rituximab before purification	% <sup>131</sup> I-Rituximab after purification
1	95.2	99.6*	95.7	99.3
2	93.9	99.6*	79.7	98.9
3	90.9	98.7	86.9	99.3
4	95.5	98.8*	95.1	99.4
5†	87.3	98.5	89.4	98.8
6†	87.3	99.4	84.6	99.4
Mean ± SD	91.8 ± 3.6	99.1 ± 0.5	88.6 ± 6.2	99.2 ± 0.3

\*Labeling prepared for clinical use.

†Day on which labeling B was performed before labeling A.

Average values before purification were used to calculate the probability of incorporated iodine atoms per molecule antibody as shown in Figure 3.

### Predictive Iodination and Radioiodination Distribution Statistics

A predictive statistical distribution of the probability of iodine incorporation based on Equation 1 (gaussian distribution) was performed, using the average number of iodine atoms per mAb molecule: 0.87 for labeling A and 0.17 for labeling B (Fig. 3). The results showed that a high percentage of polyiodinated antibodies (<sup>127</sup>I and <sup>131</sup>I) was present in labeling A, whereas the percentage was lower in labeling B.

In a second step, the probability of radioiodination of mono- and polyiodinated antibodies was calculated (Table 3; Fig. 4). The data showed that the radiolabeling probability almost doubled and tripled for biiodinated antibodies and triiodinated antibodies, respectively, compared with the probability for monoiodinated antibodies.

Finally, the probability of mono- and polyiodinated antibodies was multiplied by the probability of their being radiolabeled to obtain the probability of occurrence of radiolabeled mono- and polyiodinated antibodies (Table 3; Fig. 4). The predicted fractions calculated for polyiodinated radiolabeled antibodies were 57.3% and 15.4% for labelings A and B, respectively, if the total radiolabeled fraction of antibodies was set at 100%.

### DISCUSSION

Retention of the full immunoreactivity of a radiolabeled antibody is a primary condition for optimal tumor targeting (8,12). The use of radiolabeled antibodies that are not immunocompetent contributes to nonspecific irradiation of the

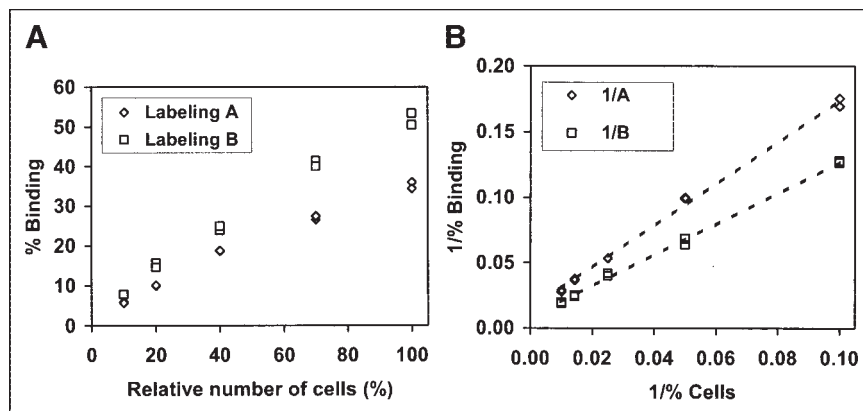
**TABLE 2**  
Specific Tracer Binding on 10<sup>7</sup> Fresh Raji or Daudi Cells and Extrapolated Maximal Binding at Infinite Antigen Excess According to Lindmo et al. (10)

Paired labeling no.	Specific binding on 10 <sup>7</sup> cells (% of input activity)				Extrapolated maximal binding (%)			
	Raji		Daudi		Raji		Daudi	
	A	B	A	B	A	B	A	B
1	25.8	41.6	52.9	59.7	36.5	66.2	61.4	68.0
2	35.3	42.2	43.3	52.3	64.9	85.5	66.2	96.2
3	23.9	59.5	25.1	58.3	65.8	100	84.0	100
4	35.2	51.9	30.8	43.4	70.4	100	65.8	100
5	54.7	59.2	59.7	67.5	89.3	95.2	100	100
6	39.7	53.6	39.9	61.1	100	100	62.9	100
Mean ± SD	35.8 ± 11.1	51.3 ± 7.9	42.0 ± 13.0	57.1 ± 8.3	71.2 ± 22.1	91.2 ± 13.5	73.4 ± 15.4	94.0 ± 12.8
Relative binding increase* (%)	43		36		28		28	
P	0.018 (n = 6)		0.016 (n = 6)		0.018 (n = 6)		0.022 (n = 6)	
	<0.001 (n = 12)				<0.001 (n = 12)			

\*Relative mean binding increase of labeling B compared with A (A = 100%).

†Calculated for paired, specific binding results of labelings A and B using the Student *t* test.

**FIGURE 2.** (A) Specific binding results (duplicates) for 5 concentrations of fresh Raji cells (dilutions between  $10^6$  and  $10^7$  cells; nonspecific binding has been subtracted). Data are from paired labeling 4. (B) Extrapolation to infinite antigen excess according to Lindmo et al. (11). In the Lindmo extrapolation, the linear regression of labeling A follows the equation  $y = 1.6032x + 0.0142$ , that of labeling B,  $y = 1.1884x + 0.0083$  (correlation coefficients for both were  $r^2 = 0.997$ ).



patient but does not contribute to specific irradiation of the tumor.

We present the results of a comparative labeling study starting with 2 different specific activities of  $^{131}\text{I}$ -rituximab, with one of the labelings being performed in the framework of a clinical study. Preparative work had been done to optimize the chemical labeling conditions using chloramine T. Residual iodine and chloramine T were eliminated by push filtration through an anion-exchange column. This represents a potential advantage over conventional labeling procedures, which commonly add the reducing agent sodium bisulfite to stop the oxidation reaction. These reducing agents can also contribute to a loss of immunoreactivity in antibodies (12).  $^{131}\text{I}$ -Rituximab, prepared in this way, resulted in  $>98.4\%$  radiochemical purity without formation of aggregates or degradation products.

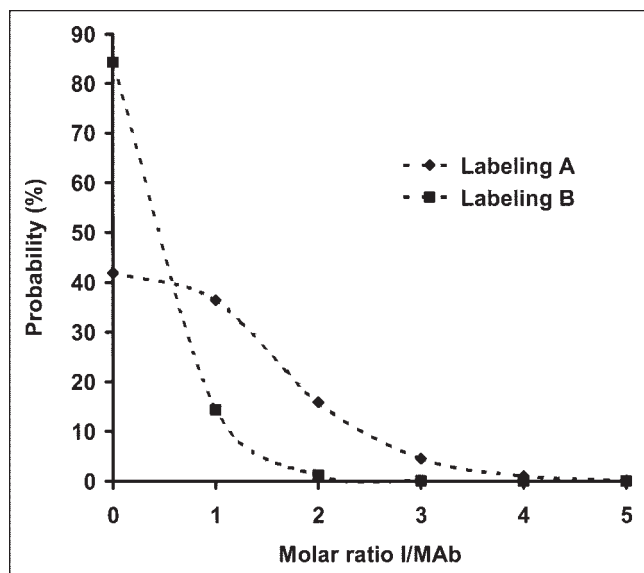


**FIGURE 3.** Probability of incorporation of one or more iodine atoms ( $^{131}\text{I}$  and  $^{127}\text{I}$ ) per antibody molecule for the average I/mAb molar ratios of 0.87 (labeling A) and 0.17 (labeling B). Probability values were calculated according to Equation 1 (gaussian distribution).

In the direct-binding assay, we measured the immunoreactivity of the radiolabeled antibody fraction, which is notably the fraction that will provide the radioimmunotherapy effect. In our opinion, immunoreactivity measured by competition assay might be biased by the presence of high percentages of unlabeled antibodies, as we found for labeling B, in which 84% of antibodies are predicted not to be iodinated. As an example, in a competition assay using  $^{111}\text{In}$ -labeled rituximab, the binding of  $^{111}\text{In}$ -rituximab would be competing with unlabeled and radioiodinated rituximab. Thus, in such a competition assay the presence of 84% noniodinated antibodies in labeling B could mask impaired immunoreactivity in the radiolabeled antibody fraction.

Impairment of immunoreactivity can result from multiple parameters such as chemicals or impurities of iodine. Furthermore, the specifications of  $^{131}\text{I}$  can vary among different producers, production methods, and batches from the same producer. Abundant tyrosine residues in the antibody complementarity-determining regions of the binding site (13) can significantly affect the immunoreactivity of radioiodinated antibodies. Measurement of immunoreactivity using live cells might further lead to variations, since cells might express variable amounts of the target antigen (CD20). Despite the varied binding results observed in our study, the use of paired labelings with the same batches of  $^{131}\text{I}$  and cells and simultaneous binding measurements allowed observation of strictly comparable conditions. Our results showed that labeling B gave a very high immunoreactivity, with a mean of  $>91\%$  at infinite antigen excess and with most of these labelings extrapolating to 100% immunoreactivity. This high immunoreactivity demonstrates that the chemical labeling conditions for both labeling A and labeling B had been close to optimal. The observation, however, of particularly low binding results or, alternatively, of very high results also for labeling A (paired labeling 5) could possibly be explained by variations in the specific activity of  $^{131}\text{I}$ .

As shown further, the strictly paired comparisons, using identical amounts of antibody rituximab, showed that label-

TABLE 3

Calculated Radioiodinated Fractions of Antibodies for Different Numbers of Iodine Atoms per mAb Molecule

No. of iodine atoms	Iodination probability* ( $P_i(x)$ )	Relative iodination probability† (%)	Radiolabeling probability‡ ( $P_a(x)$ )	Radioiodinated fraction§ ( $F(x)$ )	Relative radioiodinated fraction¶ (%)
Labeling A					
1	0.3645	62.7	0.0455	0.01658	42.7
2	0.1586	27.3	0.0888	0.01408	36.3
3	0.0460	7.9	0.1303	0.00599	15.5
4	0.0100	1.7	0.1698	0.00170	4.4
5	0.0017	0.3	0.2075	0.00035	0.9
6	0.0003	0.1	0.2436	0.00007	0.2
Labeling B					
1	0.1413	91.6	0.0455	0.00643	84.6
2	0.0122	7.9	0.0888	0.00108	14.2
3	0.0007	0.5	0.1303	0.00009	1.2

\*Calculated probability (according to Equation 1) of mono- and polyiodinated antibody fractions  $P_i(x)$ .

†Mono- and polyiodinated fractions (%) of all iodinated antibodies.

‡Respective probability to be radiolabeled  $P_a(x)$  (according to the Newton binome).§Resulting fraction (by multiplication of  $P_i(x)$  with  $P_a(x)$ ) of radiolabeled mono- and polyiodinated antibodies  $F(x)$ .

¶The later fraction (%) of all radiolabeled antibodies.

ing B gave a significantly higher immunoreactivity than did labeling A. Similar observations of higher immunoreactivity at a lower specific activity of  $^{131}\text{I}$  (29.6 MBq/mg, compared with 325.6 MBq/mg) have been described for another anti-CD20 antibody: anti-B1 (14). In another study, 11 of 12 tested antibodies showed similar results for immunoreactiv-

ity impairment at a moderate iodination degree, as was used in our study for labeling A (9). Finally, 25% immunoreactivity impairment at an I/mAb molar ratio of 1:1 had also been observed on the humanized antibody HuM195 (13). These results had already demonstrated the possible dependence of immunoreactivity on specific activity, exceptions being, however, possible. Thus, optimization of labeling is required for each antibody, especially if higher degrees of iodination are envisaged.

The presented 2-step predictive statistical distribution of mono- compared with polyiodinated antibodies showed that the percentage of polyiodinated radiolabeled antibodies was 15.4% in labeling B and 57.3% in labeling A, when setting the total number of radioiodinated antibodies at 100%. This difference of polyiodinated, radiolabeled antibodies might explain the different immunoreactivities of the 2 labelings. Using the same calculation method, it could be predicted that a radiolabeling of 1 mg of antibody with 370 MBq of  $^{131}\text{I}$  antibody of the same specific activity as used in our study would lead to a polyradioiodinated fraction of 82%. In these calculations, it was assumed that the declared specific activity of  $^{131}\text{I}$  was always reached. Generally, this parameter is not controlled by the laboratory radiolabeling the antibodies. Delivery of a lower specific activity, or use of  $^{131}\text{I}$  later than on the calibration date, would further increase the rate of polyiodination of antibodies and possibly contribute to immunoreactivity impairment.

Other parameters than those explored here could further modulate the predicted distribution probability of mono- and polyiodinated antibodies. The number of tyrosine residues is not unlimited in an antibody, and tyrosines in the

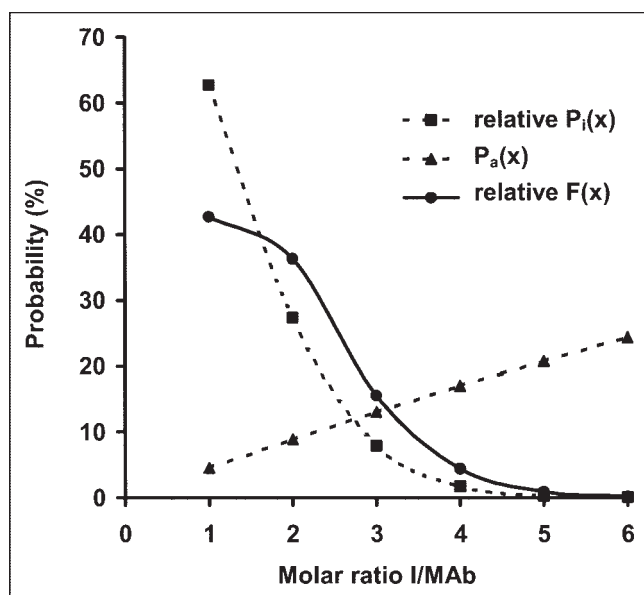


**FIGURE 4.** Development of the probability of radioiodination of mono- and polyiodinated antibodies  $F(x)$  for labeling A. Calculation is based on the relative iodination probability  $P_i(x)$  (excluding the fraction of noniodinated antibodies), the radiolabeling probability  $P_a(x)$ , and the combination of the 2 probabilities. The polyiodinated radiolabeled antibody fraction  $F(x)$  is seen to increase relative to the predicted iodination probability  $P_i(x)$ .

binding site might be preferentially labeled (13). A potential preferential radioiodination in the binding site could further reduce immunoreactivity, especially in combination with a high probability of polyiodinated radiolabeled antibodies.

Furthermore, polyradiolabeled antibodies present a higher counting rate than do monoradioiodinated antibodies. Because we radiolabeled rituximab at a low specific activity, and because polyradioiodinated antibodies are rare for  $^{131}\text{I}$  of the given specific activity, we think that these other parameters only slightly affected the results and can therefore be neglected.

By analogy, the same calculation method used for mono- and polyderivatized antibodies might also apply to most radiometal labelings. The degree of chelates per antibody would define the number of potential radiolabeling sites, and the purity of commercially available radiometals, the radiolabeling degree. Commercially available radiometals frequently contain other metal impurities that can be chelated and therefore can determine the radiolabeling degree of mono- and polychelated antibodies.

## CONCLUSION

We showed that we could preserve a high immunoreactivity for rituximab when radiolabeling at a low specific activity that resulted in a predicted molar ratio of 0.17 iodines per antibody. Furthermore, calculation of the statistical distribution probability predicted that even at the modest degree of iodination for labeling A—0.87 iodine atoms per antibody—most radiolabeled antibodies contained 2 or more iodine atoms, possibly explaining the partial loss of immunoreactivity. The presented method of calculating statistical probabilities of radiolabeling might also be relevant for radiometal-labeled antibodies and might allow prediction of the relative frequency of radiolabeled mono- and polychelated antibodies.

## ACKNOWLEDGMENT

We thankfully acknowledge support by the Swiss Cancer League (grant KFS 991-02-2000).

## REFERENCES

- Berinstein NL, Grillo-Lopez AJ, White CA, et al. Association of serum rituximab (IDEC-C2B8) concentration and anti-tumor response in the treatment of recurrent low-grade or follicular non-Hodgkin's lymphoma. *Ann Oncol*. 1998;9:995–1001.
- Leget GA, Czuczman MS. Use of rituximab, the new FDA-approved antibody. *Curr Opin Oncol*. 1998;10:548–551.
- McLaughlin P, White CA, Grillo-Lopez AJ, Maloney DG. Clinical status and optimal use of rituximab for B-cell lymphomas. *Oncology*. 1998;12:1763–1769.
- Behr TM, Wormann B, Gramatzki M, et al. Low- versus high-dose radioimmunotherapy with humanized anti-CD22 or chimeric anti-CD20 antibodies in a broad spectrum of B cell-associated malignancies. *Clin Cancer Res*. 1999;5:3304s–3314s.
- Behr TM, Griesinger F, Riggert J, et al. High-dose myeloablative radioimmunotherapy of mantle cell non-Hodgkin lymphoma with iodine-131-labeled chimeric anti-CD-20 antibody C2B8 and autologous stem cell report: results of a pilot study. *Cancer*. 2002;94:1363–1372.
- Matzku S, Kirchgessner H, Nissen M. Iodination of monoclonal IgG antibodies at a sub-stoichiometric level: immunoreactivity changes related to the site of iodine incorporation. *Int J Rad Appl Instrum B*. 1987;14:451–457.
- Eary JF, Press OW, Badger CC, et al. Imaging and treatment of B-cell lymphoma. *J Nucl Med*. 1990;31:1257–1268.
- Antonescu C, Buchegger F, Kosinski M, et al. Biokinetics of multiple doses of [ $^{131}\text{I}$ ] labelled and unlabelled chimeric anti-CD20 antibody (rituximab) in patients with non-Hodgkin's lymphoma (NHL) [abstract]. *Eur J Nucl Med*. 2002;29(suppl):S149.
- Larson SM. A tentative biological model for the localization of radiolabelled antibody in tumor: the importance of immunoreactivity. *Int J Rad Appl Instrum B*. 1986;13:393–399.
- Flieger D, Renoth S, Beier I, Sauerbruch T, Schmidt-Wolf I. Mechanism of cytotoxicity induced by chimeric mouse human monoclonal antibody IDEC-C2B8 in CD20-expressing lymphoma cell lines. *Cell Immunol*. 2000;204:55–63.
- Lindmo T, Boven E, Cuttitta F, Fedorko J, Bunn PA Jr. Determination of the immunoreactive fraction of radiolabeled monoclonal antibodies by linear extrapolation to binding at infinite antigen excess. *J Immunol Methods*. 1984;72:77–89.
- Visser GW, Klok RP, Gebbinck JW, ter Linden T, van Dongen GA, Molthoff CF. Optimal quality ( $^{131}\text{I}$ )-monoclonal antibodies on high-dose labeling in a large reaction volume and temporarily coating the antibody with IODO-GEN. *J Nucl Med*. 2001;42:509–519.
- Nikula TK, Bocchia M, Curcio MJ, et al. Impact of the high tyrosine fraction in complementarity determining regions: measured and predicted effects of radioiodination on IgG immunoreactivity. *Mol Immunol*. 1995;32:865–872.
- Kaminski MS, Zasadny KR, Francis IR, et al. Radioimmunotherapy of B-cell lymphoma with [ $^{131}\text{I}$ ]anti-B1 (anti-CD20) antibody. *N Engl J Med*. 1993;329:459–465.



The Journal of  
NUCLEAR MEDICINE

## **$^{131}\text{I}$ -Rituximab: Relationship Between Immunoreactivity and Specific Activity**

Andreas O. Schaffland, Franz Buchegger, Marek Kosinski, Cristian Antonescu, Corinne Paschoud, Carine Grannavel, Raimo Pellikka and Angelika Bischof Delaloye

*J Nucl Med.* 2004;45:1784-1790.

---

This article and updated information are available at:  
<http://jnm.snmjournals.org/content/45/10/1784>

---

Information about reproducing figures, tables, or other portions of this article can be found online at:  
<http://jnm.snmjournals.org/site/misc/permission.xhtml>

Information about subscriptions to JNM can be found at:  
<http://jnm.snmjournals.org/site/subscriptions/online.xhtml>

*The Journal of Nuclear Medicine* is published monthly.  
SNMMI | Society of Nuclear Medicine and Molecular Imaging  
1850 Samuel Morse Drive, Reston, VA 20190.  
(Print ISSN: 0161-5505, Online ISSN: 2159-662X)

© Copyright 2004 SNMMI; all rights reserved.

The logo for the Society of Nuclear Medicine and Molecular Imaging (SNMMI) features the letters 'S', 'N', 'M', and 'I' in white, arranged in a 2x2 grid within a red square background.  
SOCIETY OF  
NUCLEAR MEDICINE  
AND MOLECULAR IMAGING